ELSEVIER

Biophysical Chemistry 54 (1995) 49–60

Biophysical Chemistry

Molecular dynamics of amphotericin B I. Single molecule in vacuum and water

Jan Mazerski *, Edward Borowski

Department of Pharmaceutical Technology and Biochemistry, Technical University of Gdansk, PL 80-952 Gdansk, Poland

Received 25 May 1994; revised 20 September 1994; accepted 21 September 1994

Abstract

Molecular dynamics simulations were performed for an antifungal polyene antibiotic amphotericin B (AMB). A single molecule of the AMB was modeled in vacuum as well as in water. In the latter case it was surrounded by 354 SPC water molecules and a periodic boundary condition was applied. An amino-sugar mycosamine ring was found to be rigid in the conditions studied. The mean orientation of this ring in relation to a macrolide ring was found to be common in both simulations and similar to that observed in a crystal of N-iodoacetyl derivative. A large flexibility of the amino-sugar orientation was observed in vacuum in contrast to water simulation. Several conformers of the macrolide ring were observed in vacuum as well as in water simulation. Interactions which may force these conformational transitions have been proposed. The structuring of the water molecules around polar and ionizable parts of the AMB molecule were analysed. The influence of the dynamic behavior of the AMB on structures of supramolecular complexes containing this antibiotic is discussed.

Keywords: Molecular dynamics simulations; Antifungal antibiotic; Amphotericin B; Solvation effects; Conformational changes; Structuring of water molecules

1. Introduction.

Amphotericin B (AMB) is a polyene macrolide antifungal antibiotic produced by *Streptomyces nodosus*. AMB and other polyene antibiotics are potent agents against yeasts and pathogenic moulds. The biological activity of AMB is based on its complexation to membrane located sterols (for a revue see [1]).

The molecular structure of AMB is characterised by a heptane chromophore included in the macrolactone (macrolide) ring linked to the amino-sugar mycosamine through a glycosidic bond (Fig. 1). The molecule is of amphipatic character, with a hydrophobic polyenic chromophore facing a hydrophilic part containing several hydroxyl groups and a polar head formed by a carboxylate anion attached to the macrolide ring and the ammonium cation of the mycosamine moiety.

The structure of AMB was determined by Borowski et al. [2]. An absolute configuration of 14 asymmetric centers, configuration of the polyene chromophore as well as pyranose conformation of the amino-sugar were determined by X-ray analysis of the monocrystal of N-iodoacetylamphotericin B [3,4]. This study revealed also that in the structure of

* Corresponding author.

SSDI 0301-4622(94)00114-6

the AMB derivative a six-membered hemiketal ring formed from a ketone group at C13 and the hydroxyl group at C17 exists. X-ray results have given a good insight into the 3D compactness and the conformational possibilities of the molecule in the solid state. But possible conformations of the unsubstituted molecule in aqueous solution or in biological media under various intermolecular interactions have not been determined. The problem has been partially solved by Sowinski et al. [5] by NMR analysis. ^{1}H NMR data for amphotericin B methoxycarbonylmethylamide extracted from DQF-COSY, ROESY, and 1D spectra were compared with X-ray data. The conformation in solution was identical with that found in the crystal. However, this result was also obtained for derivatives with a changed ionic state of the polar head of the molecule. In addition, spectra were recorded in a pyridine–methanol mixture, the solvent system far from water or a biological media.

Due to the weak solubility of free amphotericin B in water as well as its tendency to aggregation [6], there is little chance of obtaining experimental results concerning the conformation of this compound under physiological conditions. For this reason a computational approach has been used to simulate the influence of solvent [7] or derivatization [8]. To get a better understanding of the influence of a solvent on the 3D structure of AMB, a series of theoretical conformational investigations with different values of dielectric constant ϵ were carried out on an isolated molecule by Rinnert and Maigret [7]. The results obtained showed that modifications of the ϵ value did not affect the conformation of the lactone ring. This may suggest that there is only one low-energy conformation of the lactone ring and that this conformation is practically identical with that obtained from X-ray analysis. Conformational energy maps of the relative orientation of the amino-sugar were also calculated and clearly indicated that only one restricted area of the conformational space is allowed in the AMB molecule. The unique energy minimum obtained from these energy maps was very close to that found in the crystalline state whatever the value given to the dielectric constant ϵ. Thus we have put forward the hypothesis that the conformational behaviour of AMB can be seen as being independent of the electrical state of the molecule itself as well as of its surrounding medium. All the studies concerning molecular models of AMB–sterol complex have been based on this hypothesis [9–12]. Conformational analysis of the relative position of the amino-sugar moiety in AMB and its methyl ester in the presence of water molecules also confirmed this hypothesis [8]. The derivatization of the carboxyl group modifies a network of hydrogen bonds around the polar head of the molecule but does not affect the orientation of the amino-sugar.

All the computational results to date concern only static structures of the antibiotic. For this reason we have begun a set of calculations to determine the dynamic behaviour of the molecule of AMB. These studies should provide information about the flexibility and conformational fluctuations of the molecule. Such information is indispensable for the design of a dynamic model of the antibiotic–sterol supramolecular complex. This complex is formed in lipidic membranes in the presence of sterol molecules. A dynamic simulation in vacuum seems to be an appropriate model of such a lipophilic environment. However, according to the standard model of the supramolecular complex, proposed by De Kruijff and Demel [9], an aqueous pore is formed in the mem-

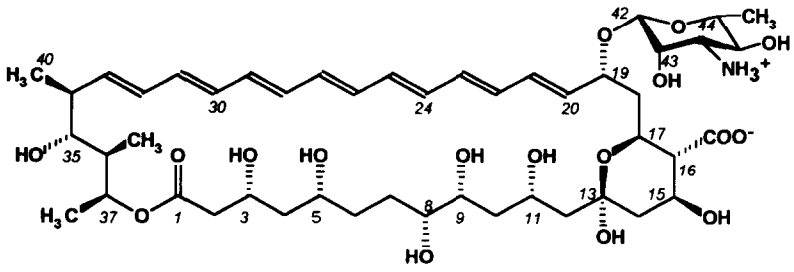

Fig. 1. Chemical structure of amphotericin B.

brane. In addition, the AMB molecules interact with membrane existing in the aqueous environment. In such a situation it is important to know the behaviour of the antibiotic molecule in the presence of water. Consequently, a dynamic simulation in water should be also performed. A comparison of the results obtained from simulations in vacuum and in water is the subject of the present paper.

2. Procedures

For the energy minimalizations and molecular dynamics simulations the GROMOS software package was used (W.F. van Gunsteren and H.J.C. Berendsen, BIOMOS B.V., Laboratory for Physical Chemistry, University of Groningen, The Netherlands). The integration of the classical equations of motion carried out with a time step of 0.5 fs without any constraints of molecular geometry. The temperature was kept at 300 K by coupling the kinetic energy of the system to a heat bath with a relaxation time of 100 fs [13]. The energy function was composed of bonding terms representing internal topology as bond lengths, bond angles, torsion angles, improper dihedrals, as well as non-bonded terms consisting of Van der Waals interactions and electrostatic contributions. For all calculations, the standard GROMOS force field was used. No explicit hydrogen bond function was employed in this force field.

The initial coordinates for the antibiotic molecule were obtained from atomic X-ray coordinates for heavy atoms [4]. The AMB molecule was in a form of zwitter-ion with dissociated carboxyl and protonated amino group. Hydrogen atoms bound to the carbon atoms were considered as 'united atom' representations. Hydrogens bound to oxygen and nitrogen atoms were placed following the standard geometry of hydroxyl group and ammonium cation, respectively.

In the case of a vacuum simulation no periodic boundary condition was employed. In the case of simulation in water the initial coordinates for the system were prepared by superimposing the crystallographic coordinates for AMB upon the coordinates of a 'well-aged' rectangular box of water molecules equilibrated in a previous simulation of pure SPC water. These water molecules with oxygen atoms whose Van der Waals radii overlapped any atoms in the AMB molecule were then discarded from the system, leaving 354 water molecules and 1 solute molecule. The box edges were set at values of 3.64, 2.06, and 1.60 nm to give the desired distance between any of the antibiotic atoms and the nearest box wall (0.5 nm). Minimum image periodic boundary conditions were employed, and interactions between molecules greater than 0.8 nm apart were truncated.

In both cases (vacuum and water) the list of non-bonded neighbours was updated every 10 MD steps. The systems were equilibrated for 5 ps to relax any artificial starting conditions produced by the initialization procedure, with periodic scaling of the atomic velocities after each 0.5 ps period if the temperature deviated from the desired value of 300 K by more than 10°. Such a protocol has been used to shorten the equilibration period [14,15]. Following the equilibration period, the simulation was continued for an additional 40 ps.

3. Results

Analysis of the energies of both systems during simulations indicated their stability. No systematic drift nor jump changes of total as well as potential energies were observed. Thus, results presented in this paper related to the equilibrium behaviour of the studied molecule.

3.1. Conformations of AMB

Mean structures obtained from vacuum and water simulations were compared on a basis of their dynamically averaged dihedral and bond angles. Amino-sugar ring structures were found to be nearly identical in both simulations and similar to their structure in the crystal.

The macrolide ring was more flexible and sensitive to the type of environment than the sugar ring. Values of five dihedral angles in both simulations were found to be significantly different from respective values in the crystal structure (angles O37–C1–C2–C3, C5–C6–C7–C8, C7–C8–C9–C10, C18–C19–C20–C21, and C36–C37–O37–C1 in vacuum simulation and angles O37–C1–C2–C3, C2–C3–

C4–C5, C3–C4–C5–C6, C9–C10–C11–C12, and C36–C37–O37–C1 in water one). The values of angles O37–C1–C2–C3 and C36–C37–O37–C1 were similar in both simulations. These two angles define the orientation of the ester group in relation to the rest of the ring. The variations of these dihedrals are relatively high but transitions between different conformers were not observed.

Analysis of the values of six remaining angles as a function of time (Fig. 2) indicated that deviation of these values from values in the crystal as well as very large fluctuations resulted from transitions between two conformations. The mean values of the dihedral angles for both conformers are presented in Table 1. It is noticeable that for each angle one of the conformers is similar to the conformer detected in the crystal.

In vacuum simulated new conformers obtained after transitions of angles C5–C6–C7–C8 and/or C7–C8–C9–C10 (Fig. 3c and d) were able to form additional hydrogen bonds with 8-OH group. One may expect that the increase of the energy due to these transitions was equalised by the energy of the hydrogen bonds (see Section 3.2). The transitions of the dihedral angle C18–C19–C20–C21 (Fig. 3b and d) were in our opinion a result of vehement motions of the amino-sugar moiety (see below).

In the simulation of the dynamic behaviour of AMB surrounded by water molecules new conformers obtained after transitions of angles: C2–C3–C4–

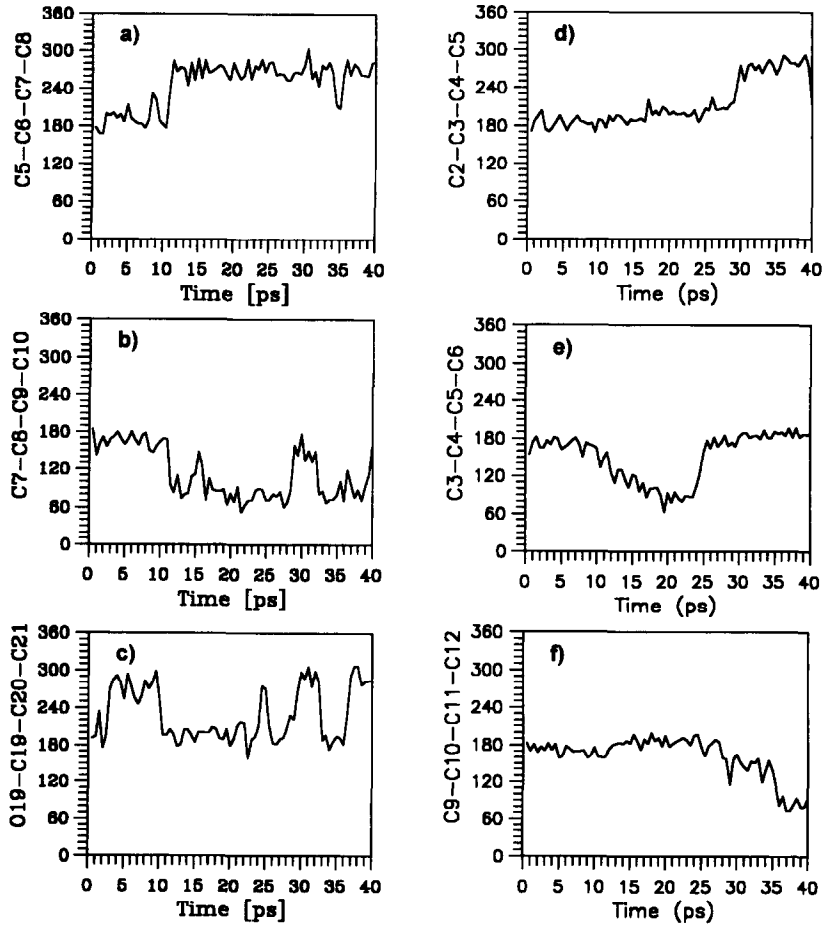

Fig. 2. Histories of the selected dihedral angles of the macrolide ring over 40 ps of the simulations: (a, b, c) in vacuum, (d, e, f) in water.

C5 (Fig. 3f), C3–C4–C5–C6 (Fig. 3e), and C9–C10–C11–C12 (Fig. 3g) were stabilized by hydrogen bonds between antibiotic hydroxyl groups and water molecules (see Section 3.2.).

It is noteworthy that all transitions during vacuum simulation were rapid in both directions. In contrast, transitions in water were rather asymmetric. For example, Fig. 2c, angle C3–C4–C5–C6 needed about 7 ps for changing from the crystal conformer ($\phi \approx 180°$) to the new one ($\phi \approx 90°$), but only about 1 ps for the reverse change. The same can be observed in the case of the dihedral angle C9–C10–C11–C12 (Fig. 2f).

The X-ray data [4] as well as results of the theoretical calculations [7] indicated that the macrolide ring in the AMB molecule is rectangular in shape. Two variables: (i) the length of the ring defined as a distance from C16 to C35 (Fig. 1), and (ii) the width of the ring defined as a distance from C8 to C24 have been selected as indicators of the shape changes. Fig. 4. illustrates the histories of these indicators during the dynamics simulations in different environments. As can be seen in Fig. 4 the mean dimensions of the macrolide ring were very similar in both the simulated environments. The variability of the dimensions in vacuum simulation

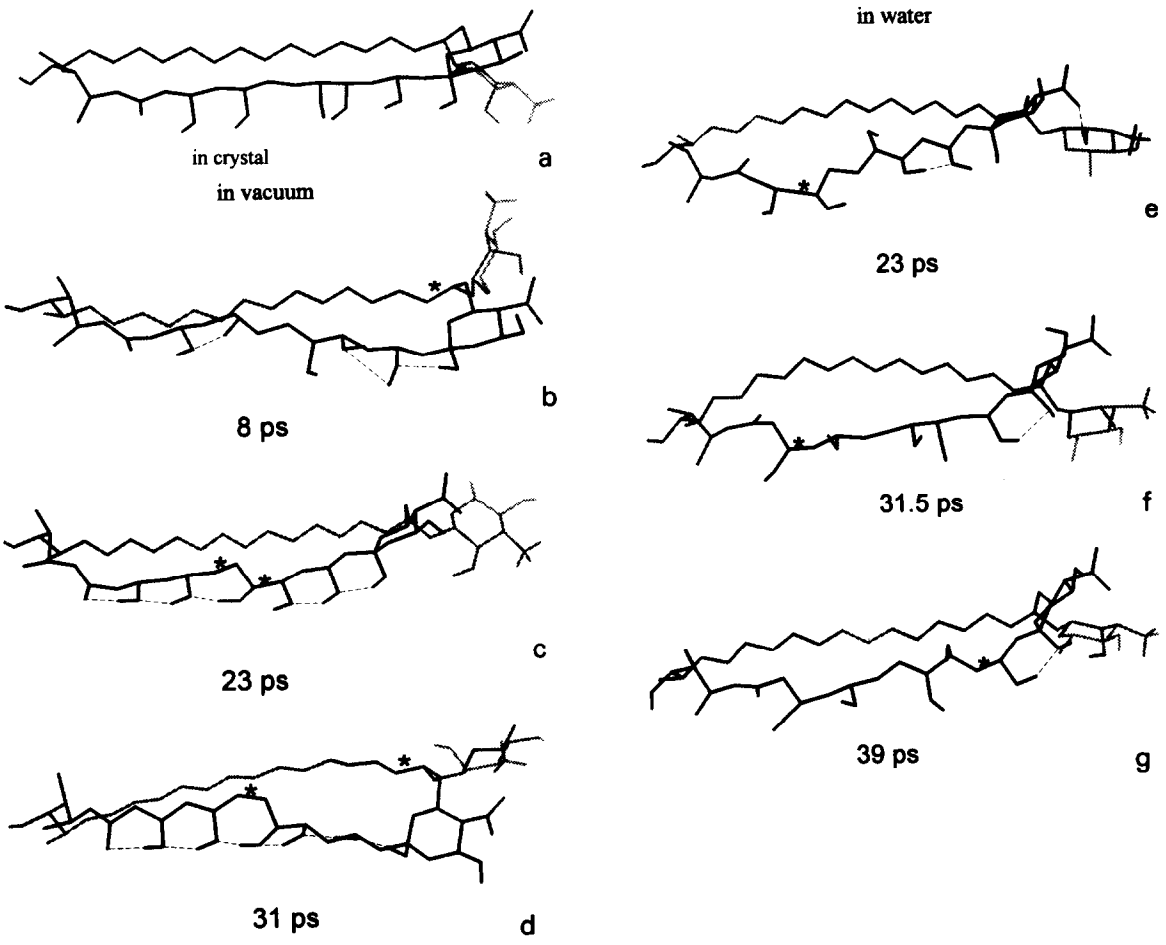

Fig. 3. Representative conformers of the macrolide ring: (a) in crystal [4], (b, c, d) during vacuum simulation, (e, f, g) during water simulation. The bond in which the dihedral angle differs from the crystal conformation is marked by an asterisk.

Table 1
Comparison of values of selected dihedral angles of the macrolide ring as calculated from vacuum and water simulations

Angle	Vacuum		Water		Crystal [7]
	Dynamical mean	RMS fluct.	Dynamical mean	RMS fluct.	
O37–C1–C2–C3	−141.3	23.8	127.9	26.6	−162.1
C2–C3–C4–C5	−177.4	10.1	−145.2	37.3	−175.9
			−86.0	*11.8*	
			−167.3	*11.7*	
C3–C4–C5–C6	178.4	10.6	151.3	178.4	
			90.5	*11.2*	
			177.5	*10.6*	
C5–C6–C7–C8	−112.5	37.3	−175.8	18.5	−169.7
	−89.9	*12.2*			
	−172.7	*11.5*			
C7–C8–C9–C10	114.1	40.6	−176.8	11.8	−177.0
	82.6	*14.2*			
	162.0	*13.8*			
C9–C10–C11–C12	175.8	11.0	161.3	32.7	183.1
			84.3	*8.8*	
			178.7	*10.6*	
C18–C19–C20–C21	109.8	43.1	72.8	11.2	101.2
	75.9	*13.4*			
	160.4	*16.2*			
C36–C37–O37–C1	−109.2	19.4	−91.6	11.3	−140.9

Dynamically-averaged values of other dihedral angles defining the geometry of the macrolide ring are the same during simulation in vacuum and water as well as being equal to values determined in the crystal [4].

was larger then in water. The variability in length was significantly lower than that in width. This observation may indicate that a relatively rigid system of seven conjugated double-bonds in *all-trans* configuration determines the shape of the macrolide ring.

The relative orientation of the amino-sugar moiety is determined by: (i) bond angle C19–O19–C42, (ii) dihedral angle C20–C19–O19–C42, and (iii) dihedral angle C19–O19–C42–O42. As can be seen from Table 2 the value of the bond angle on glycoside oxygen O19 is practically constant and environment independent. Thus, the dynamics of the amino-sugar orientation is determined by the variation of the above-mentioned dihedral angles. As can be seen from Table 2 the mean values of both angles were environmental independent and close to X-ray data. The range of fluctuations of both angles delimits the area of the phase space allowed for mycosamine. For both simulations this area was topologically connected (data not shown) indicating that in vacuum as well as in water the mycosamine moiety had only one orientation in relation to the macrolide ring. The dynamically averaged orientations from both simulations were similar and not very different from the orientation in the crystal of

Table 2
Comparison of the dynamically-averaged relative orientation of the mycosamine moiety as calculated from vacuum and water simulations

Angle	Vacuum		Water		Crystal [7]
	Dynamical mean	RMS fluct.	Dynamical mean	RMS fluct.	
C19–O19–C42	113.8	5.3	111.6	4.1	114.8
C20–C19–O19–C42	122.9	24.3	140.2	15.4	146.7
C19–O19–C42–O42	−76.0	46.6	−96.4	18.5	−100.4

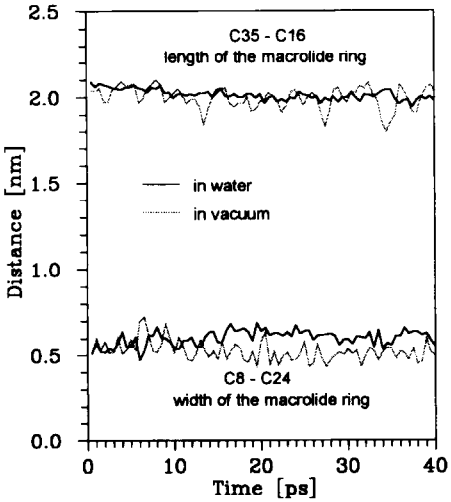

Fig. 4. Histories of the macrolide ring shape indicators over 40 ps of the simulations.

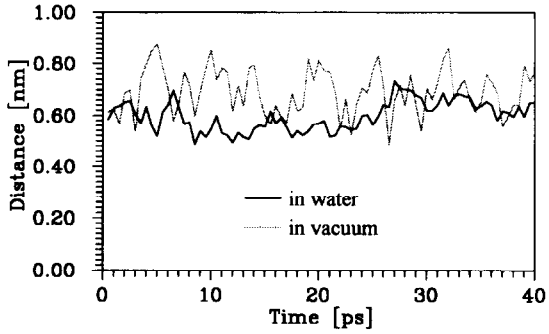

Fig. 5. History of the distance between the carboxyl carbon atom C41 and ammonium nitrogen atom N44 over 40 ps of the simulations.

the N-iodoacetyl derivative. However, the permitted area in vacuum was significantly larger than in water.

Herve et al. [10] have postulated that the distance between ammonium nitrogen and dissociated carboxyl group plays an important role in the formation of the AMB–sterol primary complex. This distance depends not only on the amino-sugar orientation but also on conformational changes of both the mycosamine and hemiketal rings. Moreover, it even depends on the sum of a lot of small changes in lengths and angles of bonds. The histories of this distance for 40 ps for both simulations are illustrated in Fig. 5.

3.2. Network of hydrogen bonds

Table 3 presents the intramolecular hydrogen bonds observed during the simulations. The hydrogen bonds in vacuum simulation were relatively stable. Four of them had a cumulative proportion of occurrence higher than 70% of the simulation period. One can see in Table 3 the unexpected behaviour of the 'equatorial' 8-OH group. Results obtained to date [4,7] suggest that this group can not form intramolecular hydrogen bonds. Transitions of dihedral angles C5–C6–C7–C8 and/or C7–C8–C9–C10 observed during simulation in vacuum allowed this group to form hydrogen bonds with O5 as well as with H9. Intramolecular hydrogen bonds in vacuum simulation formed characteristic chains (Fig. 3c): O8–H8 → O5–H5 → O3–H3 → O1 and O13–H13 → O11–H11 → O9. Rotation of groups 9-OH and 11-OH also permitted the formation of an inverted chain: O9–H9 → O11–H11 → O13. Results presented in Table 3 indicate that this inverted chain played only a minor role. Transitions of the above-mentioned dihedral angles created a certain conformation of the polar side of the macrolide ring. In this conformation a long chain of 6 hydrogen bonds including all six hydroxyl groups (from 13-OH to 3-OH) as well as carbonyl oxygen O1 could be formed (Fig. 3d).

Table 3
Intramolecular hydrogen bonds as calculated from vacuum and water simulations

Hydrogen bond	Cumulative occurrence in % of simulation period	
	In vacuum	In water
O3–H3 → O1	47.5	
O5–H5 → O3	97.5	17.5
O8–H8 → O5	71.3	
O9–H9 → O8	12.5	
O9–H9 → O11	17.5	46.3
O11–H11 → O9	73.8	
O11–H11 → O13	10.0	20.0
O13–H13 → O11	72.5	
O15–H15 → O411	2.5	
O43–H43 → O412	2.5	15.0

Table 4
Numbers of water molecules formed hydrogen bonds with amphotericin B for more than 10% of simulation time

AMB atom	Water molecule	
	As acceptor	As donor
O1		*36* 180 207 294
O3	268	**59** 172
O5	4 *36* *133*	11 246 315
O8	44	21 57 102 ***133***
O9	54 **63**	**59** ***133*** 144
O11	***47*** **63** ***148***	*148*
O13	***47*** ***148***	***47*** 56 **323**
O15	*23* *236*	**323** 332
O17		96
O19		***47***
O35	283	232 347
O411		9 ***23*** ***48*** 62 79 **93** 116 141 150 *236*
O412		***23*** ***48*** 73 **93** 163 287 *350*
O42		322
O43	325 *350*	25
N44	20 *48* 89 125	
O45	66 *335*	*335*

Bold-face numbers indicate that the water molecule interacted with more than one AMB polar group. *Italic* numbers indicate that the water molecule played the role of both acceptor and donor. ***Bold-face italic numbers*** indicate both conditions.

Intramolecular hydrogen bonds in the presence of water molecules did not occur regularly and they were not stable: formation of intermolecular hydrogen bonds was preferred (Table 4). The formation of these bonds was supported by conformational changes of the macrolide ring (Fig. 3e–g). In new conformers hydroxyl groups were more easily approachable by water molecules. From the results shown in Table 4 it can be seen that some water molecules interacted with more than one polar group of the antibiotic. In Table 4 the numbers of these molecules are shown in bold type. For example water with No. **59** played the role of donor for hydrogen bonds with O3 as well as with O9. There were also water molecules which played the role of acceptor and donor. The numbers of such molecules are shown in italics. Particularly interesting behaviour was exhibited by water molecule No. *48*. It acted as an acceptor in the hydrogen bond N44–H44 $\rightarrow O^{48}$ but also as a donor in bonds O^{48}–$H^{48} \rightarrow$ O411 and O^{48}–$H^{48} \rightarrow$ O412. The hydrogen bonds formed by this water molecule together with the intramolecular bond O43–H43 → O412 (Table 3) resulted in stabilizing the orientation of the amino-sugar moiety. Also the relatively low variability of the distance between the nitrogen and the carboxyl groups during simulation in water (Fig. 5) can be explained by those interactions.

3.3. Hydration shell around AMB molecule

The solvation requirements of the different functional groups in the AMB molecule have a strong structuring effect upon the immediately adjacent water molecules in the solution. Fig. 6 illustrates the radial distribution functions (RDF) defined as [16]:

$$\mathrm{RDF} = \frac{1}{4\pi\rho r^2}\frac{\mathrm{d}N(r)}{\mathrm{d}r}$$

where $N(r)$ is the number of water molecules at the interatomic distance r from the selected atom in the AMB molecule and ρ is the bulk water molecule number density. As would be expected, the RDF for water molecules around the methyl carbon atom C40, shown in Fig. 6a, exhibit non-polar hydration behavior, with a broad first peak centered at 0.31 and 0.33 nm for water hydrogen and oxygen, respectively. These distances are approximately equal to the Van der Waals contact distances. Similar distributions were found for other methyl groups as well as carbon atoms forming the chromophore.

In sharp contrast, the distribution of water atoms around the hydroxyl groups display the hydrogen-bonding behavior expected for these groups. Fig. 6b and c illustrate an example of these distributions for the 8-OH group. The first maximum of water oxygen–hydroxyl hydrogen RDF (Fig. 6b) at 0.18 nm is much sharper and narrower than that of the non-polar curve. The first minimum of this curve at 0.24 nm is extremely low and corresponds with a broad but evident maximum of the water hydrogen density. Distribution functions for O8 are also very characteristic. The first maximum of water hydrogen at 0.18 nm is evident but unexpectedly low (RDF ≈ 0.8). Also the second maximum at 0.32 is low (RDF ≈ 1) but higher than the first one. Such a pattern of water hydrogen density distribution may indicate that water molecules may reach the antibiotic oxygen atom only with difficulty. The RDFs for other hydroxyl

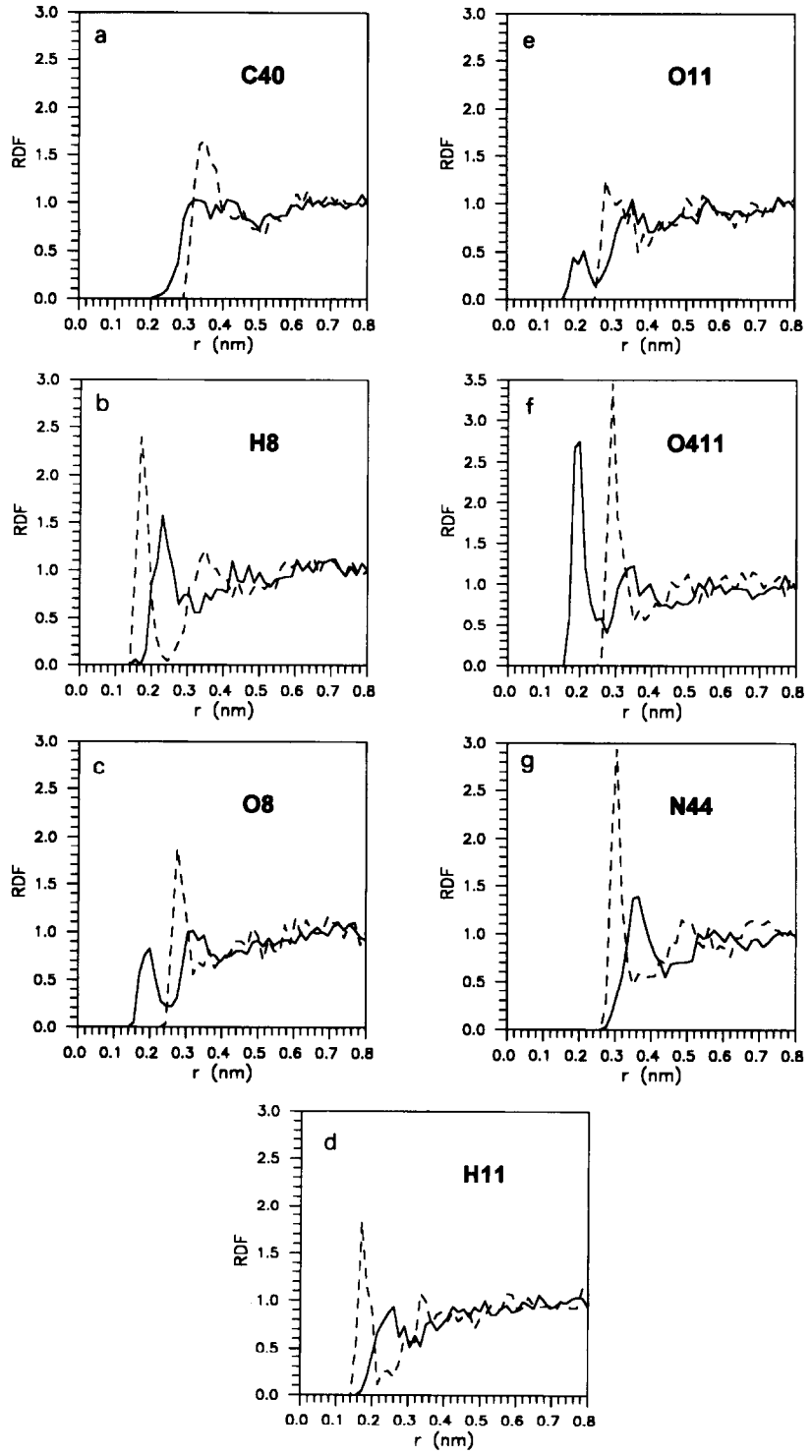

Fig. 6. Radial distribution functions of the relative density of the water atoms for selected AMB atoms. Solid and dashed lines represent RDFs of water hydrogen and oxygen atoms, respectively.

groups in the AMB molecule are generally similar to that for 8-OH but tend to have somewhat perturbed forms. Particularly high perturbation is observed for the 11-OH and 13-OH groups. Fig. 6d and e illustrate RDFs for the 11-OH group as an example. The distribution functions for H11 are generally similar to that for H8 however maxima are not so high. Distributions for O11 are different. The water hydrogen distribution exhibits a relatively low first peak (RDF ≈ 0.5). This peak may be interpreted (Fig. 6e) as a doublet with maxima at 0.18 and 0.22 nm. The second maximum is only slightly marked. Also water oxygen distribution for O11 is perturbed and diminished. In our opinion these deformations of the distributions arise from the higher steric hindrance for 'axial' (11-OH) than for 'equatorial' (8-OH) hydroxyl groups. The RDF curves for all the hydroxyl groups indicate that during the simulation these groups serve once as hydrogen bond donors and a second time as acceptors.

Particularly strong structuring effects can be observed for charged groups. Fig. 6f illustrates RDFs for one of the carboxyl oxygen atom: O411. The first peak of the water hydrogen atoms density at 0.18 nm is much higher (RDF ≈ 2.7) than that of the RDF for O8 (RDF ≈ 0.8). The first minimum of this curve at 0.26 nm corresponds with an extremely high and sharp first maximum of the water oxygen density. At 0.33–0.38 nm one can see the second maximum of the water hydrogen density which corresponds with the minimum water oxygen density. The structuring effect of O411 could be observed up to 0.5 nm from the center of this oxygen atom. Such a long-range effect indicates the important role of electrostatic interactions in the formation of the hydration shell around the carboxyl group. The structuring effect observed for the positively charged nitrogen atom N44 has also a long-range character (Fig. 6g). Of course the orientation of this shell is opposite to the shell for the negatively charged carboxyl group. The above results show that the AMB molecule in water is surrounded by a hydration shell which differs in its order of structuring degree and orientation. The highly structured, double-layer shell surrounds the ionizable head of the molecule. A less structured, monolayer shell is formed around the polyol part of the amino-sugar and the macrolide ring. The chromophore and C36–C37 fragment of the macrolide ring hardly do not induce the formation of the hydration shell.

4. Discussion

The mean structure of the amino-sugar ring in the simulations, as measured by its dynamically averaged dihedral and bond angles, was found to be practically the same in vacuum and water and very similar to that determined by X-ray diffraction. While the amino-sugar ring was found to be rigid, a few conformers of the macrolide ring were identified during the vacuum as well as solution simulations. The possibility that the macrolide ring of AMB could exist at room temperature in more than one conformation was not experimentally evidenced. The conformers detected during vacuum simulation after transition of dihedral angles C5–C6–C7–C8 and/or C7–C8–C9–C10 were stabilized by the formation of new intramolecular hydrogen bond(s) by the 'equatorial' 8–OH group. Thus, these conformers are probably formed only in conditions in which the 8–OH group can not form intermolecular hydrogen bonds. For this reason such conformers could not be detected in either crystal [4] or NMR experiments [5]. Also in the conformational analysis of Rinnert and Maigret [7] such a possibility could not be detected. The authors of this analysis used a certain type of double-step algorithm for optimizing the geometry of the macrolide ring. At the first step dihedral angles of the ring-forming bonds were optimized. At the next step only dihedrals of the hydroxyl groups were optimized. This algorithm was not able to create new conformations stabilized by intramolecular bonds (Fig. 3, Table 3). The conformational changes during water simulation are, in our opinion, forced to occur by the increased approachability of the oxygen atoms of the 'axial' hydroxyl groups to the water molecules. In part these conformers could also be stabilized by water molecules interacting with more than one hydroxyl group of the antibiotic (Table 4).

It is interesting to note that the dynamically averaged orientation of the mycosanine moiety in relation to the macrolide ring in the water solution was similar to that observed in both the vacuum and

crystal simulations. This result supports the hypothesis of Rinnert and Maigret [7] that the relative orientation of the amino-sugar moiety in the AMB molecule is independent of environmental changes as well as of chemical modifications. In the vacuum simulation a high variability of dihedrals C20–C19–O19–C42 and C19–O19–C42–O42 was observed. However, this variability was not the result of transition between different conformers. It rather indicates that an almost free change of the dihedral could occur in the interval of 100° (bond C19–O19) or 250° (bond O19–C42). In water simulation the twisting of these bonds was more restricted. The orientation is stabilized by interactions between the amino-sugar functional groups and groups attached to the macrolide ring. These interactions include direct bonding (hydrogen bond between the 43-OH and carboxyl groups, Table 3) as well as interactions mediated by the water molecules (Table 4, molecule Nos. 48 and 350). It is noticeable that such water-mediated interactions have been postulated by Meddeb et al. [8] on the basis of quantum-chemistry calculations. The pattern of water-mediated hydrogen bonds postulated by Meddeb was not exactly the same as that identified by us in the simulation, but the general features are the same: the 43-OH group as well as the 44-NH_3^+ group form, together with water molecules, chains of hydrogen bonds stabilizing the orientation of the amino-sugar.

The significance of these hydrogen-bond chains in the formation of AMB–sterol primary complex has been postulated [10,17]. A 3-β-OH group of the sterol molecule may play the role of the mediator in this interaction. The distance between both charged groups is one of the determinants of the interaction. The direct hydrogen bond N44–H44 → O44 may only exists if the distance is lower than 0.5 nm. The interaction mediated by water or the sterol OH group may exists up to 0.7 nm. The occurrence of longer distances indicates a lack of interaction between both groups. As can be seen from Fig. 5 the distance during vacuum simulation fluctuated between 0.5 and 0.9 nm with a mean value at about 0.7 nm. During water simulation fluctuations in the distance were lower and occurred between 0.5 and 0.7 nm. Such behavior indicates that both groups cannot approach each other sufficiently tightly to form a direct hydrogen bond. In contrast, the distance suitable for water (hydroxyl)-mediated interaction was easily achieved in both simulations.

The absence of a hydration shell around the chromophore fragment of the antibiotic molecule forces it to take part in the hydrophobic interaction. This interaction could be a driving force in:

(1) the formation of aggregates in the aqueous media [6],

(2) interaction with biological and lipidic membranes, and

(3) the formation of complexes with sterol in hydroalcoholic media [18,19].

The formation of aqueous pores in sterol-containing membranes also results from the lack of a hydration shell around part of the molecule.

The fact that the macrolide ring of the AMB was conformationally flexible is the crucial conclusion of this paper. While the general shape of the molecule was rather conserved during the simulations the macrolide ring was able to dynamically change the conformation of its parts. The macrolide ring was able to form a few different conformations depending on the driving force. When intermolecular hydrogen bonds cannot be formed, conformers with an increased number of intramolecular ones are preferred. In contrast, the formation of intermolecular hydrogen bonds prefers conformations in which such bonds are more easily formed. Such flexibility of the macrolide ring together with a high variability of the amino-sugar orientation may be important when an antibiotic molecule takes part in the formation of supramolecular complexes (pores). They allow the molecule to create better-packed, better-fitted and more stable structures. This fact should be taken into consideration when molecular models of antibiotic aggregates as well as of other complexes are to be studied. Further calculations may confirm the significance of the dynamic behavior of the AMB molecule for the structure of AMB including supramolecular complexes. Such calculations are currently in progress and the results will be presented in further papers in this series.

Acknowledgements

This study was supported by the State Committee for Scientific Research, Warsaw, Poland, (Grant No.

2P 303 060 06), and in part by the Faculty of Chemistry, Technical University of Gdansk.

References

[1] H.A. Gallis, R.H. Drew and W.W. Pickard, Rev. Infect. Dis., 12 (1990) 308.
[2] E. Borowski, J. Zielinski, T. Ziminski, L. Falkowski, P. Kolodziejczyk, J. Golik and E. Jereczek, Tetrahedron Lett., (1970) 3909.
[3] W. Mechlinski, C.P. Schaffner, P. Ganis and G. Avitable, Tetrahedron Lett., (1970) 3873.
[4] P. Ganis, G. Avitable, C.P. Schaffner and W. Mechlinski, J. Am. Chem. Soc., 18 (1971) 4560.
[5] P. Sowinski, J. Pawlak, E. Borowski and P. Gariboldi, Magn. Reson. Chem., 30 (1992) 275.
[6] J. Mazerski, J. Grzybowska and E. Borowski, Eur. Biophys. J., 18 (1990) 159.
[7] H. Rinnert and B. Maigret, Biochim. Biophys. Res. Comm., 101 (1981) 853.
[8] S. Meddeb, J. Berges, J. Caillet and J. Langlet, Biochim. Biophys. Acta, 1112 (1992) 266–272.
[9] B. De Kruijff and R.A. Demel, Biochim. Biophys. Acta, 339 (1974) 57.
[10] M. Herve, J.C. Debouzy, E. Borowski, B. Cybulska and C.M. Gary-Bobo, Biochim. Biophys. Acta, 980 (1989) 261.
[11] M. Bonilla-Marin, M. Moreno-Bello and I. Ortega-Blake, Biochim. Biophys. Acta, 1061 (1991) 65.
[12] V.E. Khutorsky, Biochim. Biophys. Acta, 1108 (1992) 123.
[13] H.J.C. Berendsen, J.P.M. Postma, W.F. van Gunsteren, A.D. Nola and J.R. Haak, J. Chem. Phys., 81 (1984) 3684–3690.
[14] P.H. Axelsen, C. Haydock and F.G. Prendegrast, Biophys. J., 54 (1988) 249.
[15] R.M. Venable, B.R. Brooks and F.W. Carson, Proteins, 15 (1993) 374.
[16] P.J. Rossky and M.J. Karplus, J. Am. Chem. Soc., 101 (1979) 1913.
[17] J. Mazerski, J. Bolard and E. Borowski, Proceedings of 3th International Symposium on Molecular Aspects of Chemotherapy, 19–21 June 1991, Gdansk, Poland, p. 35.
[18] I. Gruda and J. Bolard, Biochem. Cell Biol., 64 (1987) 234.
[19] J. Mazerski, J. Bolard and E. Borowski, Biochim. Biophys. Acta, in preparation.